FARADAY

Speciation modelling of the electroprecipitation of rare-earth cuprate and nickelate materials

Speciation of aqueous solutions not at equilibrium

Paul M. S. Monk,* Robert Janes and Robert D. Partridge
Department of Chemistry, Manchester Metropolitan University, Manchester, UK M1 5GD

Films of insoluble metal hydroxide have been obtained by cathodic electroprecipitation from aqueous solutions containing the nitrate salts of a lanthanide (La^{3+} or Nd^{3+}) and a transition-metal cation (Ni^{2+} or Cu^{2+}). Manipulation of deposition parameters, such as deposition voltage, V_a and solution composition, allows for extensive variation in mole fractions, x, of each metal in the final bimetallic hydroxide product. The variations in x are attributed to changes in the chemical environment within the Nernst layer at the electrode/solution interface, occurring in tandem with differences in the solution- and solid-phase speciation characteristics of the two metals and their hydroxides.

The experimentally obtained compositions of the deposited solid oxyhydroxide have been correlated with thermodynamically derived overall formation constants, β, and calculations of concentration obtained using a full speciation analysis. This model can be used to correctly predict compositions, which is taken to verify the model of electroprecipitation used.

Introduction

We have recently explored the use of electrodeposition as a means of forming films of mixed-metal oxide systems. While investigating the mechanism of electrodeposition, it was shown, for the first time, that computer speciation modelling of a system could be used to predict the composition of electrodeposited films.[1] The agreement between experiment and calculation using speciation was sufficiently good that validation of the mechanism can be assumed.

In aqueous systems containing nitrate ion, the immediate product of electrodeposition comprises both oxide and hydroxide, and is more properly termed oxyhydroxide. Electrodeposition is suited to film-formation, and in particular to the formation of thin-film electronic materials because: (a) such films have the required homogeneity owing to the atomic-level mixing of solution-phase precursors; (b) the energy demands of deposition are low, and the technique is easily adaptable to large-scale processing; (c) films can be formed on any conducting material and on non-linear substrates, or substrates which are shaped or pre-engineered to suit the practical applications of the films; (d) films have no carbon-based impurities (which is the case following the firing of many sol–gel-derived films); and (e) film-formation factors such as thickness and composition can be easily controlled by electrochemical parameters such as deposition time, current and solution composition.

There is presently great interest in the fabrication of mixed-metal oxide films with useful conducting and magnetic properties.[2–28] One of the largest areas of interest is in the formation of high T_c superconducting thin-films[2–16] for use in electronic and microwave devices. Other metal oxide materials which have applications as films include semiconductors[2] (*e.g.* TiO_2, Tl_2O_3), electrochromic materials,[18] solid oxide fuel cells,[19,20] ferroelectric materials,[21] and permanent magnets (strontium,[22] barium[23] and zinc[24] ferrites). Conventional techniques for forming such films include[25–27] sputtering, pulsed laser deposition and chemical vapour deposition. The main disadvantages of these methods are the complexity and expense of the apparatus, the high energy demands (due to the high temperatures and precise atmospheric conditions required) and the dependence of the product purity on the source materials.

The most widely used mechanism for the electrodeposition of superconductors is the simultaneous reduction of metals to form alloy films. The films are sintered to produce the required oxide superconductors. Mixed-metal films of Y–Ba–Cu, Bi–Sr–Ca–Cu and Ti–Ba–Ca–Cu have been successfully deposited with the correct stoichiometries for the formation of $YBa_2Cu_3O_{7-\delta}$, $Bi_2Sr_2Ca_2Cu_3O_{10}$ and $Tl_2Ba_2Ca_2Cu_3O_{10}$, respectively. Most depositions were formed in organic solutions[6–12] (using solvents such as DMSO and DMF) because the reduction potentials of some of the metals are too cathodic for aqueous deposition. Alloy films have also been deposited from aqueous solutions by adding complexing agents to shift the reduction potential anodically. Potentials were typically in the range −2.5–5 V. In some cases, the potential was interrupted periodically to effect pulsed currents: this was done to allow ion replenishment at the electrode/solution interface, resulting in the production of films having superior solid-state properties and improved superconducting characteristics.[6,9,12] The composition of such films was controlled by manipulating the deposition voltage and solution composition. Occasionally, complexing agents were added to solution to shift reduction potentials to achieve the target metal stoichiometries. Virtually all workers prepared deposition solutions using nitrate salts; in some cases care was taken to maintain a water-free environment by using dehydrated salts.[8–11]

Other deposition mechanisms which have been used for superconductor synthesis include: the deposition of mixed-metal hydroxides by reduction of water (from nitrate salts) in propan-2-ol;[28] deposition of mixtures of metals and hydroxides (as discussed below);[14,15] formation of metal oxide/hydroxide films by voltammetric cycling;[13] electrophoresis of metal oxide suspensions;[2–4] and mixed electrodeposition and electrophoresis.[16]

The form of electrodeposition used in this study involves the electrochemical formation of hydroxide ion by reduction of the nitrate ion in aqueous solution, and subsequent formation of insoluble films of metal hydroxide:[29]

$$NO_3^- + 7H_2O + 8e^- \rightarrow NH_4^+ + 10OH^- \quad (1)$$

$$5M^{2+} + 10OH^- \rightarrow 5M(OH)_2 \quad (2)$$

The oxide product is formed during subsequent high-

Table 1 Thermodynamic reaction processes used during the speciation analysis of the electrochemical environment, as compiled from the JESS database

log β	reaction
(i) copper species	
hydroxide species	
−9.0127	$Cu^{2+} + 2H_2O = 2H^+ + [Cu(OH)_2]_{(s)}$
−16.2000	$Cu^{2+} + 2H_2O = 2H^+ + [Cu(OH)_2]$
−39.0679	$Cu^{2+} + 4H_2O = 4H^+ + [Cu(OH)_4]^{2-}$
−26.0309	$Cu^{2+} + 3H_2O = 3H^+ + [Cu(OH)_3]^-$
−21.1254	$3Cu^{2+} + 4H_2O = 4H^+ + [Cu_3(OH)_4]^{2+}$
−7.5200	$Cu^{2+} + H_2O = H^+ + [CuOH]^+$
−10.8000	$2Cu^{2+} + 2H_2O = 2H^+ + [Cu_2(OH)_2]^{2+}$
−5.3828	$2Cu^{2+} + H_2O = H^+ + [Cu_2OH]^{3+}$
3.8395	$Cu^{2+} + H_2O = e^- = H^+ + [CuOH]_{(s)}$
nitrates	
−109.2500	$Cu^{2+} + 3H_2O + NH_3 = 8e^- + 9H^+ + [CuNO]^{2+}$
−219.9700	$Cu^{2+} + 6H_2O + 2NH_3 = 16e^- + 18H^+ + [Cu(NO_3)_2]^+$
−330.5710	$Cu^{2+} + 9H_2O + 3NH_3 = 24e^- + 27H^+ + [Cu(NO_3)_3]$
(ii) lanthanum species	
hydroxide	
−8.3161	$La^{3+} + H_2O = H^+ + [LaOH]^{2+}$
−17.6122	$La^{3+} + 2H_2O = 2H^+ + [La(OH)_2]^+$
−27.3883	$La^{3+} + 3H_2O = 3H^+ + [La(OH)_3]$
−22.7883	$La^{3+} + 3H_2O = 3H^+ + [La(OH)_3]_{(s)}$
−24.5053	$2La^{3+} + 3H_2O = 3H^+ + [La_2(OH)_3]$
−26.1852	$3La^{3+} + 3H_2O = 3H^+ + [La_3(OH)_3]$
nitrates	
−107.9220	$La^{3+} + 3H_2O + NH_3 = 8e^- + 9H^+ + [LaNO_3]^{2+}$
(iii) neodymium species	
hydroxides	
−12.1522	$2Nd^{3+} + 2H_2O = 2H^+ + [Nd_2(OH)_2]^{4+}$
−78161	$Nd^{3+} + H_2O = H^+ + [NdOH]^{2+}$
−19.3883	$Nd^{3+} + 3H_2O = 3H^+ + [Nd(OH)_3]_{(s)}$
−24.3883	$Nd^{3+} + 3H_2O = 3H^+ + [Nd(OH)_3]$
−15.9122	$Nd^{3+} + 2H_2O = 2H^+ + [Nd(OH)_2]^+$
−82.2012	$6Nd^{3+} + 12H_2O = 12H^+ + [Nd_6(OH)_{12}]^{6+}$
−55.7872	$6Nd^{3+} + 8H_2O = 8H^+ + [Nd_6(OH)_8]^{10+}$
nitrates	
−108.5900	$Nd^{3+} + 3H_2O = NH_3 = 8e^- + 9H^+ + [NdNO_3]^{2+}$
−218.5890	$Nd^{3+} + 6H_2O = 2NH_3 = 16e^- + 18H^+ + [Nd(NO_3)_2]^+$
(iv) nickel species	
hydroxides	
−12.800	$Ni^{2+} + 2H_2O = 2H^+ + [Ni(OH)_2]_{(s)}$
−9.8600	$Ni^{2+} + H_2O = H^+ + [NiOH]^+$
−19.3471	$Ni^{2+} + 2H_2O = 2H^+ + [Ni(OH)_2]$
−30.0000	$Ni^{2+} + 3H_2O = 3H^+ + [Ni(OH)_3]^-$
−30.5137	$4Ni^{2+} + 4H_2O = 4H^+ + [Ni_4(OH)_4]^{4+}$
−10.5484	$2Ni^{2+} + H_2O = H^+ + [(Ni)_2OH]^{3+}$
nitrates	
−109.3400	$Ni^{2+} + 3H_2O + NH_3 = 8e^- + 9H^+ + [NiNO_3]^+$
−219.5800	$Ni^{2+} + 6H_2O + 2NH_3 = 16e^- + 18H^+ + [Ni(NO_3)_2]^+$

Each line commences with the respective formation constant (cited as log β); such values have been corrected to zero ionic strength and to 298 K. All species are present in solution unless indicated otherwise.

temperature sintering.

These electrochemical reactions have been exploited previously, primarily to make nickel electrodes for battery applications so, in consequence, most of the reports in the literature of this reaction have focussed on nickel hydroxide formation.[30–32] Also, additional metal hydroxides have been simultaneously electrodeposited with nickel hydroxide to form composite products. A number of metal hydroxides have been co-deposited in minor amounts (typically with the second metal present in a 10% metal content).[29,33,34] Variations in the composition of mixed films with different co-metal were thought to be caused by differences in the solubility characteristics of the metal hydroxides.[29]

The electrodeposition of metal hydroxide has also been employed in our laboratories for the addition of transition metals into tungsten(VI) oxide or molybdenum(VI) oxide electrochromic thin films.[35–38] Such films were deposited from solutions containing W and Mo oxidatively 'dissolved' in hydrogen peroxide; the additional metals were added as nitrate salts. The indentity of the W and Mo solutes were not known for sure, but species of the type $[(O_2)_2{-}X{-}O{-}X{-}(O_2)_2]^{2-}$ (X = Mo, W) are thought to be in solution, with H^+ as the counter-ion.[39] We are unaware of the existence of any β values for these solutes. Whatever the solute and the mechanism of electroprecipitation, however, current passage caused the formation of films of mixed-metal

oxyhydroxide: it is considered that solid is formed *via* a combination of nitrate reduction and reduction of W and Mo complexes to cause hydroxide formation.

The application of the nitrate reduction reaction [eqn. (1) and (2)] to the preparation of superconductor films has been limited to its use in combination with alloy[15] deposition, or as a (largely overlooked) side reaction. The formation of hydroxide during alloy deposition in organic solutions has been noted to occur *via* the reduction of water[14,15] (present either as part of a solvent mixture, or from hydrated nitrate salts). However, nitrate reduction is the more likely reaction, especially for depositions at lower potentials (−1–−2 V).

In this work, the primary target material was lanthanum cuprate (La_2CuO_4), the antecedant of a range of superconducting phases; the formation of the related compounds lanthanum nickelate (La_2NiO_4) and neodymium nickelate (Nd_2NiO_4) were also studied. The preparation of neodymium cuprate (Nd_2CuO_4) has been described extensively elsewhere.[1,40]

A previous study of mixed neodymium–copper hydroxide formation showed a dependence of film composition on the thermodynamic formation characteristics of the two metal hydroxides. The correlation between composition and formation constants is discussed here for the deposition of lanthanum–copper hydroxide mixtures. A computer speciation modelling routine, which was employed in the Nd–Cu investigation,[1] is used to predict the precipitation products from thermodynamic information. These results are compared with the experimentally determined compositions.

Experimental

Electrodeposition

Deposition solutions were prepared by using aqueous metal nitrate mixtures. The concentration of each cation was 0.025 mol dm^{-3}, unless otherwise stated. The temperature of the bath solutions was maintained at 298 K. All solutions were purged with N_2 gas prior to electrodeposition.

Electrodeposition was performed using a PAR 273A potentiostat interfaced to a PC running PAR 270 electrochemistry software. Solutions were gently agitated by stirring slowly during deposition to maintain convective control. The rate of solution flow was optimised to facilitate ion replenishment at the electrode without causing film disruption or streaking, as determined using a chronoamperometric system, and the slowest stirring rate which would still prevent the current drop caused by ion depletion was determined.

Electrodeposition was performed potentiostatically using a three-electrode configuration. The working electrode was silver foil of area 4.8 cm^2, the counter-electrode was a platinum mesh of large surface area, and the reference electrode was a saturated calomel electrode (SCE). All potentials are cited with respect to the SCE. The deposition current was typically in the range 10–50 mA cm^{-2}, the value depending on the deposition conditions. The deposition time was 120 s unless stated otherwise.

Elemental analysis of films

Elemental compositions of deposited films were determined using a Philips PU 7450 inductively coupled plasma (ICP) spectrometer. Films were rinsed following deposition, and dissolved in 2 mol dm^{-3} nitric acid prior to ICP analysis.

Films were dried thoroughly prior to sintering on the electrode substrate. sintering conditions were typically 1223 K for 15 min in air. Sintered films were analysed by X-ray diffraction (XRD) and energy dispersive spectroscopy (EDS) whilst still on the electrode substrate, and were dissolved in nitric acid for elemental analysis.

X-Ray powder diffractograms were obtained using a Philips PU 3020 diffractometer operating with Cu-Kα radiation. EDS measurements were obtained using a Cambridge 250 electron microscope.

Speciation

A comprehensive list of all the species which may be formed from the ions present in the electrodeposition environment (*i.e.* Cu^{2+}, La^{3+}, H^+, NO_3^- and OH^-) was compiled from the Joint Expert Speciation System[41] (JESS) thermodynamic database. The thermodynamic constants for each of these species were also obtained from the database and their values corrected to 298 K and zero ionic strength, see Table 1. The distribution of the species as a function of solution pH values were simulated using the Equilibrium Simulation for Titration Analysis[42] (ESTA) speciation program.

The ESTA program uses an iterative procedure to solve mass-balance equations. The formation constants, β, used in the computer modelling were obtained from the JESS database (all β values are corrected to zero ionic strength and 298 K). The values of β used here are listed in Table 1. It is worth noting that the computer speciation program adopts a convention that makes the hydroxide ion (OH^-) equivalent to minus one proton ($-H^+$) according to the following rearrangement of the water-dissociation reaction

$$H_2O = H^+ + OH^- \quad \text{so} \quad H_2O - H^+ = OH^- \qquad (3)$$

This convention allows for aqueous systems to be described in terms of hydrogen ions and K_w alone. (It must be stressed that this practice is a mathematical tool only; it has no chemical meaning and is used solely to aid the computational process.)

Results

All films were amorphous as deposited, or insufficiently crystalline to allow an X-ray diffractogram to be obtained. EDS was unable to detect any material segregation, indicating that there are no 'clusters' of either metal in the deposited solid, *i.e.* that mixing of the two component metals was always complete (certainly, atomic-level mixing is present in the deposition solution). Dissolving films of varying thickness[1] also shows that the films are homogeneous as deposited.

Initially, the compositions of deposited films were determined as a function of deposition voltage, V_a, whilst using a constant deposition solution composition ($[La^{3+}] = [Cu^{2+}] = 0.025$ mol dm^{-3}). The mol fractions of La and Cu in the deposited mixed-metal oxyhydroxide films changed with deposition voltage as shown in Fig. 1; the mol fraction of La increases as V_a becomes more cathodic.

Next, films were electrodeposited from solutions made with varying ratios of La and Cu, *i.e.* keeping $[Cu^{2+}]$ constant at 0.025 mol dm^{-3} but steadily increasing the La concentration to 0.125 mol dm^{-3}. Increasing the La^{3+} concentration caused an increase in the deposition content of La. The effect of varying the ratio of cations in solution is shown in Fig. 2.

Manipulation of these two deposition parameters facilitates the extensive variation of the metal content of the deposited films, and allows film compositions to be 'tailored' to more-or-less any desired stoichiometry. The synthesis of the target material, lanthanum cuprate, La_2CuO_4, requires the deposited films to have an La : Cu mol fraction of 0.667 : 0.333. This composition (±0.005) is achieved by electrodeposition onto a silver electrode for 120 s at −1.60 V from solutions containing 0.125 mol dm^{-3} lanthanum nitrate and 0.025 mol dm^{-3} copper nitrate.

Deposition time

All films described so far were deposited during a fixed period of time (120 s). It is not uncommon for the initial current to

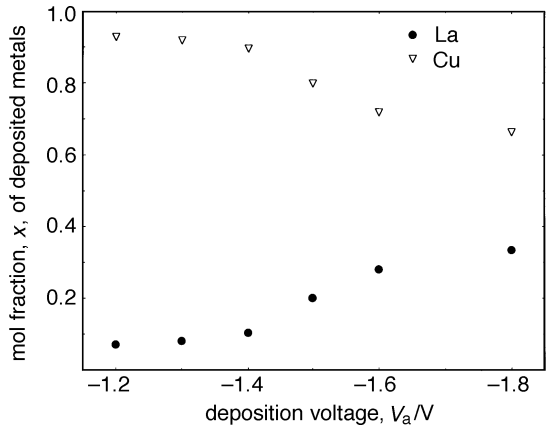

Fig. 1 Mol fraction x of La in films of La_x–Cu_{1-x}–O as a function of the deposition voltage V_a: a constant deposition solution composition ($[La^{3+}] = [Cu^{2+}] = 0.025$ mol dm^{-3}) was used throughout. All solutes were nitrate salts and no additional solutes were used; the electrode substrate was metallic silver.

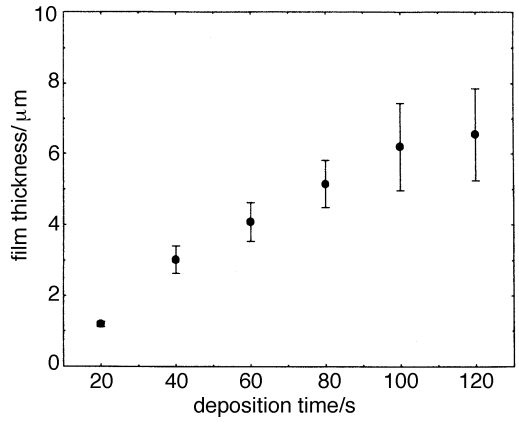

Fig. 3 Variation in film thickness as a function of deposition time at constant potential: film thickness was determined using an SEM and holding the film (on Ag) 'end on'

drop during the first few seconds of electrodeposition, caused by mass-transport limitations but, more importantly, by the formation of films which are less conducting *i.e.* films having a greater resistance, R, than does the electrode substrate. It is usual for the value of R to increase steadily during film growth, thus affecting the actual potential applied at the double layer and possibly causing film compositional changes.

Films of lanthanum cuprate were deposited using varying lengths of time (*i.e.* different amounts of charge were passed, thus leading to films having different thicknesses). For each film the ratio of La to Cu was ascertained using ICP, and the film thickness was determined (after firing) using an SEM. Fig. 3 illustrates the variation in thickness as a function of deposition time for sintered films on Ag. The plot is slightly curved: it is assumed that the gelatinous, hydrated nature of the films during deposition causes a slight but almost insignificant IR drop. Analysis of SEM micrographs showed the thickness of a related film of $NdCu_2O_4$ (deposited by a current passage of 2 min) was 6.6 μm.

The size of the IR drop was not great enough to affect film composition depositions during the 120 s of deposition since there was no variation (within experimental error) in the ratio of La to Cu with deposition time.

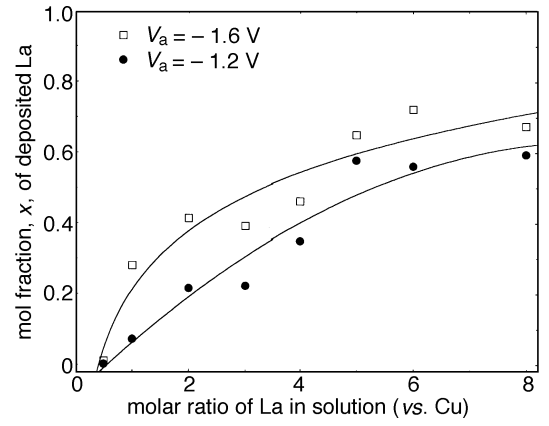

Fig. 2 Mol fraction x of La in films La_x–Cu_{1-x}–O as a function of the concentration ratio of La^{3+} to Cu^{2+} in the initial deposition solution: $[Cu^{2+}]$ was kept constant at 0.025 mol dm^{-3} but $[La^{3+}]$ was increased steadily to a limit of 0.125 mol dm^{-3}. All solutes were nitrate salts and no additional solutes were used; the electrode substrate was metallic silver.

Film firing

Films were sintered in air for 15 min. The metal content of films was confirmed by EDS and ICP analysis. There is no evidence whatsoever for inhomogeneity within electroprecipitated films following firing. The formation of the desired lanthanum cuprate phase was confirmed by XRD. Fig. 4 shows an XRD pattern for a sample of electroprecipitated La_2CuO_4 as a function of temperature. There are seen to be some impurity phases such as CuO or La_2O_3 in the electroprecipitated material at relatively low sintering temperatures but, after 15 min at $T > 800$ °C, the material is seen to be pure La_2CuO_4. The XRD for the sample contains additional peaks due to the silver substrate (as indicated by ∗).

Mechanism of electroprecipitation

The mechanism of the cathode electrodeposition process can be described as follows: the electrogeneration of hydroxide ion at the electrode/solution interface causes a localised pH increase. The rate of hydroxide generation, and therefore the rate of localised pH increase within the Nernst layer, depends

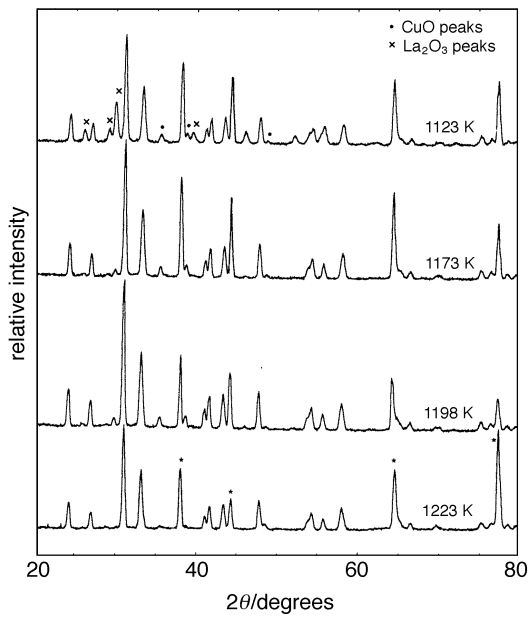

Fig. 4 XRD of electroprecipitated La_2CuO_4 on metallic silver as a function of sintering temperature. (Peaks deriving from the Ag of the substrate are represented as ∗ on the bottom trace.)

on the deposition current, I; and I is exponentially related to the deposition voltage, V_a, by the Butler–Volmer equation.[43]

Also, since OH^- is rapidly consumed by eqn. (2), there is rather a steep change or 'step' in the concentration $[OH^-]$, which falls at a distance, δ, from the electrode. Such a step in the reaction variable (here pH) is often termed a 'reaction front' since only at the front are both of the reactants (here M^{n+} and OH^-) present in comparable concentrations; $[M^{n+}] \approx 0$ between the electrode and δ and $[OH^-]$ is extremely low in the solution bulk. The interfacial pH rise depends on the distance, δ, from the electrode at which the reaction front falls (which is more-or-less constant for a steady stirring rate) and the bulk solution pH (which is constant for any given solution composition). The pHs at the electrode/solution interface have also been determined approximately in the past,[40] and such experimental values appear quite similar (to within about ± 0.5 pH units) to the thermodynamically calculated pH in Fig. 5. Considering the approximations inherent in such a measurement, the closeness of the experimental and calculated values of pH gives us confidence that the calculated values are valid.

Hydroxide ion is electrogenerated at the working electrode. The initial interfacial pH rise at the electrode causes the formation (and subsequent precipitation) of metal hydroxide species. Therefore, the actual interfacial pH has an equilibrium value, the exact pH depending on the competition of hydroxide in the precipitation reaction.

When two different metal ions are present, the composition of the electrodeposited product is governed by the thermodynamic differences between the two metal hydroxide formation reactions. The thermodynamic differences between lanthanum hydroxide formation and copper hydroxide formation have been assessed using the ESTA speciation computer program. Fig. 5 shows the calculated species concentrations in a solution containing La^{3+} and Cu^{2+} (each 0.025 mol dm^{-3}) over a range of solution pHs. This speciation distribution profile shows $Cu(OH)_{2(s)}$ formation occurs at a much lower pH than does the formation of $La(OH)_{3(s)}$, *i.e.* in a solution of gradually increasing pH, hydroxide ions are consumed in the formation of the thermodynamically preferred product $Cu(OH)_{2(s)}$, after which the remaining hydroxide ions were available for $La(OH)_{3(s)}$ formation.

It is assumed that, with hydroxide generation and the subsequent pH rise being so rapid, the rates of hydroxide formation are the same for each metal, *i.e.* virtually 'instantaneous'. Thus, the two metals are precipitated simultaneously, at an interfacial pH which is controlled by a combination of metal hydroxide thermodynamics and OH^- formation kinetics. The available OH^- is partitioned between the two metal ions and the competitive precipitation of the two metal hydroxides is thermodynamically governed.

The above description of mixed-metal hydroxide electroprecipitation can be used to explain the film compositional changes which are caused by the variation of deposition parameters. Analysis of Fig. 5 allows for verification of Fig. 1 and 2. Using the data in Fig. 5, the predicted compositional amounts of La and Cu in solid material may be determined over the speciation pH range 7–8 (Fig. 6). The mol fractions, x, in Fig. 6 are seen to correlate with the film compositional changes over the deposition voltage range -1.2–-2.0 V (see Fig. 1). Over this V_a range, the Cu deposition content remains the same and the La content progressively increases (which is equivalent to an increase in the La mol fraction and a decrease in the Cu mol fraction). A more detailed discussion of this type of correlation is discussed elsewhere for the deposition of Nd–Cu hydroxides.[1]

A series of speciation distributions similar to Fig. 5 were calculated using speciation environments corresponding to differing amounts of each cation in solution. The compositions of precipitated solid were calculated over the pH range 7–8 to enable direct comparison with the electrodeposition compositions over the V_a range -1.2–-2.0 V. All compositions are expressed as mol fractions of metal in the solid products. Fig. 7 shows the compositional trend for solutions over this pH range as a function of the ratio of solutes; Fig. 7 illustrates the compositional changes as the La solute concentration is increased. When this plot is compared to that of x *vs.* V_a (see Fig. 2), there is seen to be satisfactory agreement between experimental results and results obtained using computer speciation.

Preparation of lanthanum nickelate and neodymium nickelate

Electrodeposition was performed from aqueous solutions containing mixtures of La^{3+}–Ni^{2+} and Nd^{3+}–Ni^{2+}, each solute present as a nitrate salt. The compositions of the mixed hydroxide products were determined as a function of both deposition voltage and solution composition. As with the deposition of La–Cu products, variation in deposition parameters such as solute ratio and V_a caused variation in the composition of deposited films to an extent that the desired compositions were made.

Fig. 8 shows a speciation profile of the Nd^{3+}–Ni^{2+} system. It will be noticed that the pH range in this figure is much narrower than for the La–Cu system (see Fig. 5). This is

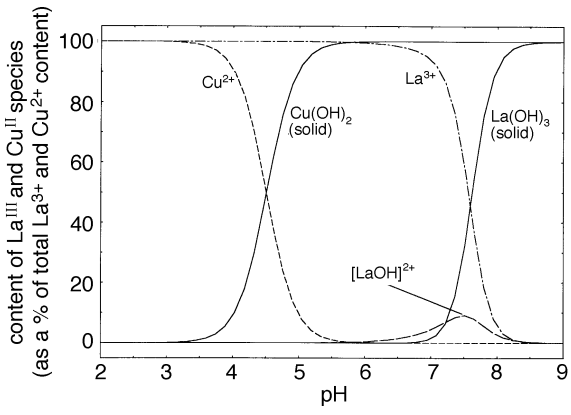

Fig. 5 Speciation distribution profile of La^{3+}, Cu^{2+} and solution-phase species derived from them, in the pH range 2–9. The total amounts of La^{3+} and Cu^{2+} equate to a concentration of 0.025 mol dm^{-3}, each solute being used as a nitrate salt. The profile was calculated using the ESTA program.

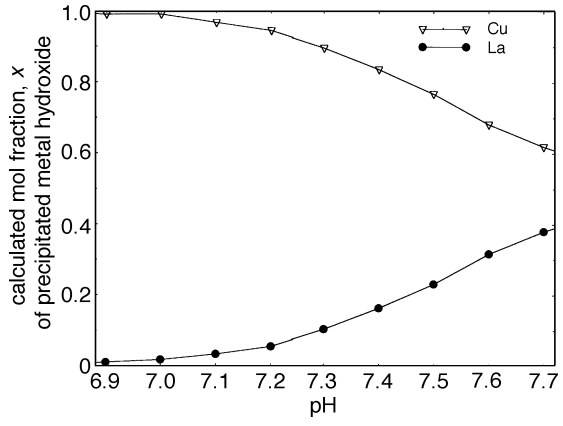

Fig. 6 Mol fractions of Cu and Ia in the mixed-metal hydroxide solid, calculated from Fig. 5 for an aqueous solution containing only $La(NO_3)_3$ and $Cu(NO_3)_2$ as precursors: the calculation assumed that precursor ions were both used at a concentration of 25 mmol dm^{-3}. Experimentally determined data for comparison are shown in Fig. 1.

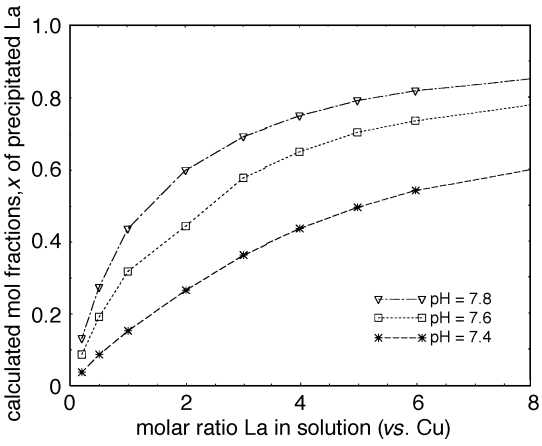

Fig. 7 Mol fractions of La in the mixed-metal hydroxide solid, calculated from speciation profiles such as that in Fig. 5. The speciation calculation assumed a solution containing only $La(NO_3)_3$ and $Cu(NO_3)_2$ as precursors: it was programmed with a constant solution phase concentration $[Cu^{2+}] = 25$ mmol dm^{-3}, and the concentration of La^{3+} was varied. Experimentally determined data for comparison are shown in Fig. 2.

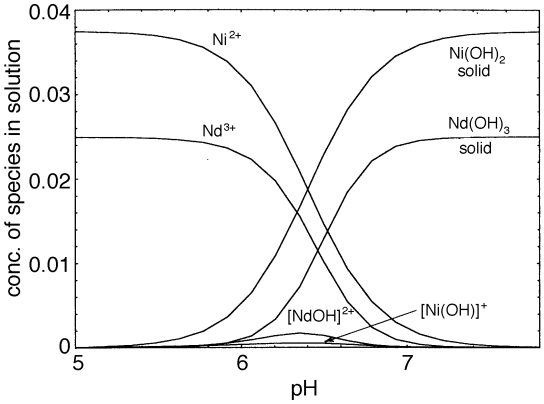

Fig. 8 Speciation distribution profile of Nd^{3+}, Ni^{2+} and solution-phase species derived from them, in the pH range 5–8. The total amount of Ni^{2+} was 0.0375 mol dm^{-3} and the total amount of Nd^{3+} was 0.025 mol dm^{-3}, each solute being present initially as a nitrate salt. The profile was calculated using the ESTA program.

because Nd and Ni hydroxides have solubility constants, K_s, which are quite similar. Experimentally, this similarity in K_s is seen when depositing mixtures of Nd–Ni hydroxide. Fig. 9 shows such a plot of the mol fraction, x, of Ni in the electrodeposited product as a function of deposition voltage for a number of different solute ratios. It is clear from this figure that there is not a wide variation in x with voltage.

Despite the narrow range of pHs in the speciation profile (Fig. 8) arising from the narrow range of V_a employed, each of the target hydroxides was prepared by electrodeposition. The deposition conditions which generate films with the target metal ratio of 2 : 1 for La : Ni and Nd : Ni hydroxide films such as follows:

$$La_2NiO_4 = -1.60 \text{ V } vs. \text{ SCE},$$

$$[La] : [Ni] = 0.04 : 0.025 \text{ mol dm}^{-3},$$

onto silver for 2 min

$$Nd_2NiO_4 = -1.60 \text{ V } vs. \text{ SCE},$$

$$[Nd] : [Ni] = 0.0375 : 0.025 \text{ mol dm}^{-3},$$

onto silver for 2 min.

Sintering of such films in air at 950 °C for 15 min results in the formation of the nickelate phase in each case. Fig. 10 and 11 show diffraction patterns of electrogenerated films of La_2NiO_4 and Nd_2NiO_4, respectively. The respective reference pattern is also shown in each figure; references were obtained from the Daresbury crystallographic database.

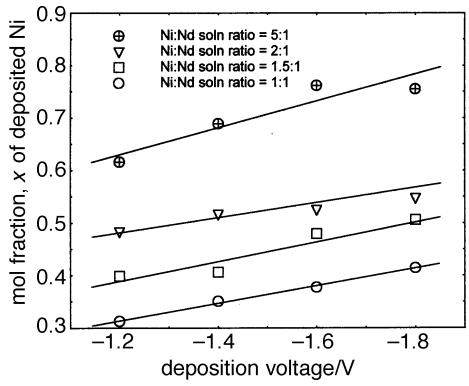

Fig. 9 Mol fraction, x, of Ni in films of Nd_x–Ni_{1-x}–O as a function of both deposition voltage V_a and concentration ratio of Ni^{2+} to Nd^{3+} in the initial deposition solution: $[Nd^{3+}]$ was kept constant at 0.025 mol dm^{-3} but $[Ni^{2+}]$ was varied. All solutes were nitrate salts and no additional solutes were used; the electrode substrate was metallic silver.

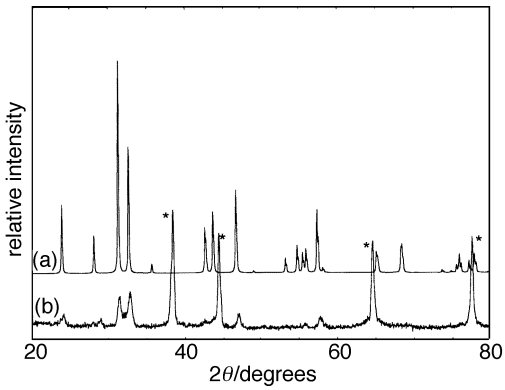

Fig. 10 XRD of $LaNiO_4$: (a) the reference XRD pattern from the Daresbury crystallographic database, and (b) the XRD of a sample electroprecipitated on metallic silver (the peaks indicated as ∗ represent the Ag substrate)

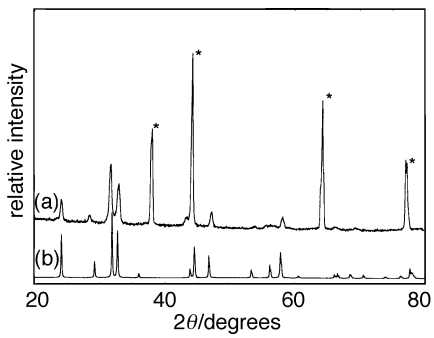

Fig. 11 XRD of Nd_2NiO_4: (a) the XRD of a sample electroprecipitated on metallic silver (the peaks indicated as ∗ represent the Ag substrate), and (b) the reference XRD pattern from the Daresbury crystallographic database.

Conclusions

It has been shown that the compositions of electroprecipitated rare-earth cuprates can be modelled using the computer-speciation programs JESS and ESTA. These programs are

usually used in conjunction with systems at equilibrium rather than pseudo-steady-state, as here. This is therefore an extension to the usual use of the computer speciation procedure. After high-temperature firing, the XRD patterns of electroprecipitated products are identical to the XRD patterns of reference materials.

Electrodeposition of La_2CuO_4 onto a silver electrode required a potential of -1.60 V *vs.* SCE and a solution comprising 0.125 mol dm^{-3} of lanthanum nitrate and 0.025 mol dm^{-3} of copper nitrate. Using this same potential and again using Ag as the electrode, La_2NiO_4 can be formed using a solution comprising [La] : [Ni] = 0.04 : 0.025 mol dm^{-3} and Nd_2NiO_4 is formed using [Nd] : [Ni] = 0.0375 : 0.025 mol dm^{-3}.

We wish to thank Mr J. A. Jarrett for help with using the JESS and ESTA programs, and Dr Brian Wardle for helpful discussions. We also thank the EPSRC for a studentship (for R.D.P.)

References

1 P. M. S. Monk, R. Janes and R. D. Partridge, *J. Chem. Soc., Faraday Trans.*, 1997, **93**, 3985.
2 C. T. Chu and B. D. Dunn, *Appl. Phys. Lett.*, 1989, **55**, 492.
3 B. Zhang, P. Fabbricatore, G. Gemme, R. Musenich, R. Parodi and L. Risso, *Physica C*, 1992, **193**, 1.
4 N. Casan-Pastor, P. Gomez-Romero, A. Fuertez and M. Brossa, *Solid State Ionics*, 1993, **66**, 241.
5 S. H. Pawar, M. M. Tonape and V. N. Shinde, *Mater. Chem. Phys.*, 1993, **35**, 86.
6 R. N. Bhattacharya and R. D. Blaugher, *Physica C*, 1994, **225**, 269.
7 S. H. Pawar and H. A. Mujawar, *Mater. Res. Bull.*, 1990, **25**, 1443.
8 M. Maxfield, H. Eckhardt, Z. Iqbal, F. Reidinger and R. H. Baughman, *Appl. Phys. Lett.*, 1989, **54**, 5940.
9 A. Weston, S. Lalvani, F. Willis and N. Ali, *J. Alloys Comp.*, 1992, **181**, 233.
10 S. Ondono-Castillo, A. Fuertes, F. Perez, P. Gomez-Romero and N. Casan-Pastor, *Chem. Mater.*, 1995, **7**, 771.
11 K. A. Richardson, D. M. W. Arrigan, P. A. J. de Groot, P. C. Lanchester and P. N. Bartlett, *Electrochim. Acta*, 1996, **41**, 1629.
12 R. N. Bhattacharya, P. A. Parilla, R. P. Noufi, P. Arendt and N. Elliott, *J. Electrochem. Soc.*, 1992, **139**, 67.
13 P. Slezak and A. Wiekowski, *J. Electrochem. Soc.*, 1991, **138**, 1038.
14 R. N. Bhattacharya and R. D. Blaugher, *Physica C*, 1994, **229**, 244.
15 H. Minoura, K. Naruto, H. Takano, E. Haseo, T. Sugiura, Y. Ueno and T. Endo, *Chem. Lett.*, 1991, **3**, 379.
16 M. Maxfield, *J. Electrochem. Soc., Extended Abstr.*, 1990, **90-1**, no. 536.
17 P. Searson, *Solar Energy Mater. Solar Cells*, 1992, **27**, 377.
18 P. M. S. Monk, R. J. Mortimer and D. R. Rosseinsky, *Electrochromism: Fundamentals and Applications*, VCH, Weinheim, 1995.
19 I. Yashuda and H. Hishinuma, *J. Electrochem. Soc.*, 1996, **143**, 1583.
20 M. Nagata and H. Irahowa, *Mater. Res. Bull.*, 1993, **28**, 255.
21 A. Atkinson and P. T. Mosely, *Appl. Surf. Sci.*, 1993, **65/66**, 212.
22 J. B. Wallace, H. W. King and E. A. Payzat, *J. Magn. Magn. Mater.*, 1993, **124**, 9.
23 K. H. Yoon, D. H. Lee, H. J. Jung and S. O. Yoon, *J. Mater. Sci.*, 1992, **27**, 2941.
24 S. Ram and J. C. Joubert, *J. Magn. Magn. Mater.*, 1991, **99**, 133.
25 D. Jedamzik, *GEC J. Res.*, 1990, **8**, 2.
26 M. R. Beasley, *Proc. IEEE*, 1989, **77**, 1155.
27 W. Kautek, *Vacuum*, 1992, **43**, 403.
28 S. B. Abolmaali and J. B. Talbot, *J. Electrochem. Soc.*, 1993, **140**, 443.
29 D. A. Corrigan and R. M. Bendert, *J. Electrochem. Soc.*, 1989, **136**, 723.
30 C. C. Streinz, A. P. Hartman, S. Motupally and J. W. Weidner, *J. Electrochem. Soc.*, 1995, **142**, 1084.
31 H. N. Seiger, and V. J. Puglisi, *Proc. Power Sources Symp.*, 1974, **26**, 115.
32 C. C. Streinz, S. Motupally and J. W. Weidner, *J. Electrochem. Soc.*, 1995, **142**, 4051.
33 D. A. Corrigan and M. K. Carpenter, *SPIE Int. Ser.*, 1990, **IS4**, 298.
34 Y. Mo, E. Hwang and D. A. Scherson, *J. Electrochem. Soc.*, 1996, **143**, 37.
35 P. M. S. Monk and S. L. Chester, *Electrochim. Acta*, 1993, **38**, 1521.
36 P. M. S. Monk, S. L. Chester, D. S. Higham and R. D. Partridge, *Electrochim. Acta*, 1994, **39**, 227.
37 P. M. S. Monk, R. D. Partridge, R. Janes and M. J. Parker, *J. Mater. Chem.*, 1994, **4**, 1071.
38 P. M. S. Monk, T. Ali and R. D. Partridge, *Solid State Ionics*, 1995, **80**, 75.
39 K. Yamanaka, H. Oakamoto, H. Kidou and T. Kudo, *Jpn. J. Appl. Phys.*, 1986, **25**, 1420.
40 R. Janes, P. M. S. Monk, R. D. Partridge and S. B. Hall, *J. Mater. Chem.*, 1996, **6**, 183.
41 P. M. May and K. Murray, *JESS Primer user manual*, 1996.
42 P. M. May and K. Murray, *ESTA version 3.0 user manual*, 1989.
43 A. J. Bard and L. R. Faulkner, *Electrochemical Methods: Fundamentals and Application*, Wiley, New York, 1980.

Paper 7/06095E; *Received* 26*th June*, 1997